Medial Collateral Ligament Insertion Site and Contact Forces in the ACL-Deficient Knee

Benjamin J. Ellis,[1] Trevor J. Lujan,[1] Michelle S. Dalton,[1] Jeffrey A. Weiss[1,2]

[1]Department of Bioengineering, University of Utah, Salt Lake City, Utah 84112

[2]Department of Orthopaedics, University of Utah, Salt Lake City, Utah 84132

Received 11 May 2005; accepted 3 October 2005

Published online 2 March 2006 in Wiley InterScience (www.interscience.wiley.com). DOI 10.1002/jor.20102

ABSTRACT: The objectives of this research were to determine the effects of anterior cruciate ligament (ACL) deficiency on medial collateral ligament (MCL) insertion site and contact forces during anterior tibial loading and valgus loading using a combined experimental-finite element (FE) approach. Our hypothesis was that ACL deficiency would increase MCL insertion site forces at the attachments to the tibia and femur and increase contact forces between the MCL and these bones. Six male knees were subjected to varus–valgus and anterior–posterior loading at flexion angles of 0° and 30°. Three-dimensional joint kinematics and MCL strains were recorded during kinematic testing. Following testing, the MCL of each knee was removed to establish a stress-free reference configuration. An FE model of the femur–MCL–tibia complex was constructed for each knee to simulate valgus rotation and anterior translation at 0° and 30°, using subject-specific bone and ligament geometry and joint kinematics. A transversely isotropic hyperelastic material model with average material coefficients taken from a previous study was used to represent the MCL. Subject-specific MCL in situ strain distributions were used in each model. Insertion site and contact forces were determined from the FE analyses. FE predictions were validated by comparing MCL fiber strains to experimental measurements. The subject-specific FE predictions of MCL fiber stretch correlated well with the experimentally measured values ($R^2 = 0.95$). ACL deficiency caused a significant increase in MCL insertion site and contact forces in response to anterior tibial loading. In contrast, ACL deficiency did not significantly increase MCL insertion site and contact forces in response to valgus loading, demonstrating that the ACL is not a restraint to valgus rotation in knees that have an intact MCL. When evaluating valgus laxity in the ACL-deficient knee, increased valgus laxity indicates a compromised MCL. © 2006 Orthopaedic Research Society. Published by Wiley Periodicals, Inc. J Orthop Res 24:800–810, 2006

Keywords: medial collateral ligament (MCL); anterior cruciate ligament (ACL); knee; finite element analysis; anterior–posterior laxity; varus–valgus laxity

INTRODUCTION

The effect of anterior cruciate ligament (ACL) deficiency on the mechanical function of other knee ligaments remains unclear, although it is known that even knees with reconstructed ACLs often exhibit abnormal knee kinematics.[1] The ACL is a primary restraint to anterior tibial translation and a secondary restraint to valgus rotation,[2–12] while the medial collateral ligament (MCL) is a primary restraint to valgus rotation[2,3,5–14] and a secondary restraint to anterior tibial translation.[2–4,8,11,14–18] The MCL is involved in approximately 40% of all severe knee injuries,[19] while approximately 50% of partial MCL tears and 80% of complete MCL tears occur in conjunction with injury to other knee ligaments.[20] In alpine skiing, the most common ligament that is injured in conjunction with the MCL is the ACL.[21]

Animal studies have shown that MCL healing is substantially poorer in the case of a combined MCL/ACL injury than for an isolated MCL injury.[2–4,7,11,12] After 12 weeks of healing, MCLs from knees with combined MCL/ACL injuries had a tensile strength of only 10% of control values.[12] It has been proposed that the healing MCL in the ACL-deficient knee is subjected to increased strains and forces as a result of ACL deficiency.[2]

Correspondence to: Jeffrey A. Weiss (Telephone: 801-587-7833; Fax: 801-585-5361; E-mail: jeff.weiss@utah.edu)

An ACL graft acts as a stabilizer initially, but as it heals, forces are transferred to the MCL that hinder healing and result in hypertrophy of the MCL with tissue of lower quality. As long as 2 years after injury, healing MCLs still had "significantly different biological composition, biomechanical properties, and matrix organization" (p. 348).[11]

Although animal studies have shown that the MCL may be at risk for injury in an ACL-deficient knee, conclusions as to the exact contributions of the MCL and ACL to valgus stability vary within and between studies of ligament healing in animal models and joint kinematics in cadaver models. In animal models, the variation in results is confounded by the variation in the type of injury model used. Results from a rabbit healing study showed that valgus rotation does not increase over time in response to healing of the ACL graft after an O'Donoghue triad injury (MCL rupture with removal of the ACL and part of the medial meniscus), although anterior translation did significantly increase over the same healing period.[4] The conclusions of this study are in contrast to other animal studies that have shown higher ACL forces and increased valgus laxity in response to a valgus load in an MCL-deficient knee.[2,3,5,6,8,9] Two previous cadaver studies concluded that valgus laxity is relatively unaffected by ACL deficiency,[13,14] and Mazzocca and colleagues concluded that, "the ACL can be compromised in isolated grade III MCL injuries" caused by a valgus load (p. 148).[9] The actual insertion site and contact forces in the MCL in response to a valgus torque in the intact and ACL-deficient knee, which arguably are the most relevant data for interpretation of ligament contribution to joint function, are unknown.

The aim of this study was to examine the effects of ACL deficiency on MCL insertion site and contact forces when the knee is subjected to anterior tibial loading and valgus torque. We hypothesized that ACL deficiency would cause an increase in MCL insertion site and contact forces in response to both loading conditions.

METHODS

Overview

We combined experimental and computational methods to determine the effect of ACL injury on MCL insertion site and contact forces during anterior tibial loading and valgus loading. Computed tomography (CT) images were used to obtain subject-specific geometry for the femur, tibia, and MCL in six cadaveric knees. Each knee was tested with the ACL intact and then with the ACL transected. For both conditions, the knee was subjected to anterior–posterior (A-P) translation and varus–valgus (V-V) rotation at two flexion angles (0° and 30°) with tibial rotation constrained and unconstrained while knee kinematics and MCL strains were recorded. Polygonal surfaces were extracted from the CT data and used to generate subject-specific FE models. The models were analyzed under the experimentally measured kinematics to determine MCL strains, contact forces, and insertion site forces. FE-predicted fiber stretches were compared to experimental values as a means of validation, and the effects of injury state, flexion angle, and tibial constraint on MCL insertion site and contact forces were determined.

Specimen Preparation and CT Scan

The six intact cadaver knees were from males with a mean age of 60 ± 8.3 years. Preparation for testing followed the same protocol as Gardiner and colleagues,[22] with the exception that additional contrast markers were used to define gauge lengths for measurement of MCL fiber strains. Markers were distributed along the visible fiber direction in a 3×7 grid pattern, forming 18 gauge lengths (Fig. 1). Each gauge length was approximately 15 mm long. The marker positions were chosen based on anatomical landmarks. The boundaries of the femoral and tibial MCL insertion sites were marked with copper wires to aid in identifying their geometry in the volumetric CT images. Nylon kinematic blocks were fastened to the distal femur and proximal tibia (Fig. 1), while positioning blocks with three beveled cavities (not shown), forming a right angle, were fastened to the proximal femur and distal tibia.[23] After dissection, a volumetric CT scan was obtained for each knee at 0° flexion (slice thickness = 1.3 mm with 1.0 mm overlap, 142–168 mm field of view, and 512×512 acquisition matrix).

Kinematic Testing

Following the CT scan, each knee was mounted in fixtures on a custom materials testing machine, which allowed both A-P translation and V-V rotation to be applied at fixed flexion angles with constrained or unconstrained tibial axial rotation and unconstrained medial–lateral translation and joint distraction (Fig. 2). During testing, 10 cycles of A-P translation (load limits of ±100 N at 1.5 mm/s) and 10 cycles of V-V rotation (torque limits of ±10 N-m at 1 d°/s) were independently applied to the tibia. The A-P load and V-V torque limits were established to be large enough to achieve the terminal stiffness of the ligament without inflicting injury to the tissue and thereby allowing multiple tests with the same specimen.[24] A-P and V-V loading were

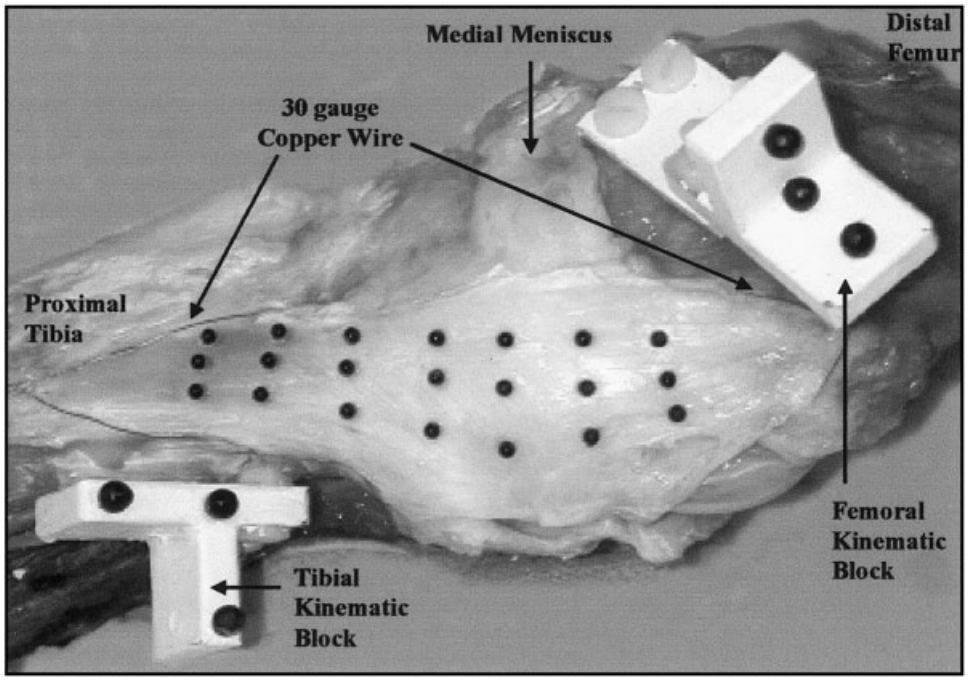

Figure 1. Photograph of test setup for simultaneous measurement of MCL strain and knee joint kinematics. Twenty-one markers (2.38 mm diameter) defined 18 regions for strain measurement. Kinematic blocks were used to measure tibiofemoral kinematics during testing. Femoral and tibial kinematic blocks, each with three contrast markers (4.75 mm diameter), were affixed to the cortical bone. The kinematic blocks were used to measure tibiofemoral kinematics and to register the CT data with the configuration of the knee during experimental testing. Insertion sites were marked with 30-gauge copper wire.

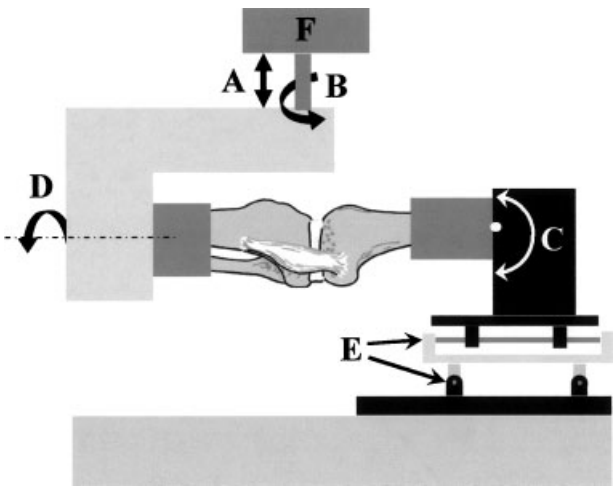

Figure 2. Schematic of the loading apparatus, depicting a medial view of the knee at 0° flexion. (A) Applied A-P translation. (B) Applied V-V rotation. (C) Adjustable flexion angle. (D) Constrained or unconstrained tibial axial rotation. (E) Unconstrained medial–lateral translation and joint distraction. (F) Load/torque cell.

conducted at 0° and 30° flexion. The tests were repeated with tibial axial rotation constrained and unconstrained at each flexion angle. The load and torque were measured with a multi-axis load cell (Futek T5105, Irvine, CA; accuracy ±2.2 N and ±0.056 N-m).

Following the intact tests, the ACL was transected through the midsubstance without damage to the PCL or removal of the knee from the fixture, and all the tests were repeated. Finally, following ACL transection, the attachment of the medial meniscus to the MCL was transected. This test was performed to verify that the attachment did not influence joint kinematics and MCL strains under A-P and V-V loading; a similar conclusion was reached for the effect of the meniscal attachment on MCL strains in the intact knee in our previous study.[22] To minimize hysteresis effects, data from the 10th cycle of loading were analyzed for all tests.

Care was taken to ensure that the relative positions of the bones were duplicated for a given flexion angle and tibial axial rotation constraint for both injury states. When testing the intact knee, a neutral A-P and V-V position was determined at each flexion angle with tibial axial rotation unconstrained. The neutral A-P and V-V positions were determined by iteratively adjusting the

 DOI 10.1002/jor

starting position and running A-P and V-V motion cycles until the given load and torque limits produced equal anterior and posterior translation and equal varus and valgus rotations, respectively. Once these reference positions were established, actuator translation and rotation positions were logged so the positions could be restored after ACL transection. The three-dimensional (3D) kinematic position of the femur relative to the tibia was verified through the use of a Microscribe digitizer (Immersion Corp., San Jose, CA; accuracy ±0.085 mm) in combination with the positioning blocks. The digitizer and positioning blocks were used to precisely determine the relative 3D kinematics of the femur and tibia.[25] In this manner, positional repeatability between tests was insured.

Measurement of Joint Kinematics and Ligament Strains

A digital motion analysis system consisting of two high-resolution digital cameras (Pulnix TM-1040, 1024 × 1024 × 30 fps, Sunnyvale, CA) and Digital Motion Analysis Software (DMAS, Spica Technology Corporation, Maui, HI) was used to record MCL strain in the 18 measurement regions and joint kinematics simultaneously (strain measurement accuracy ±0.035%; joint kinematic translational accuracy ±0.025 mm; joint kinematic rotational accuracy ±0.124°).[23]

In Situ Strain

At the conclusion of testing, the MCL was dissected from the bones and placed in a buffered saline bath for 10 min to allow the ligament to achieve a stress-free reference configuration. The 3D coordinates of the fiducial markers on the MCL were determined using the digital motion analysis system. This provided reference (zero-load) lengths for each strain region, l_o.[12,22,26] These values were combined with length measurements taken during the kinematic testing to calculate in situ fiber strain between marker pairs. These data were used as input to the subject-specific FE models.[22,27]

CT Scan, Surface Reconstruction, and FE Mesh Generation

Using the copper insertion site wires and MCL strain contrast markers as guides, cross-sectional contours of the MCL, femur, and tibia were extracted from the CT dataset (SurfDriver, Kailua, HI). Polygonal surfaces were generated by stacking and lacing together the contours,[28] and smoothing was applied.[29] The polygons composing the surfaces of the femur and tibia were converted directly to shell elements and used to represent the bones as rigid bodies.[30] The MCL surface was imported into FE preprocessing software (TrueGrid, XYZ Scientific, Livermore, CA), and a hexahedral mesh was created.

Constitutive Model

The MCL was represented as transversely isotropic hyperelastic, with the strain energy (W)[22]:

$$W = F_1(\tilde{I}_1) + F_2(\tilde{\lambda}) + \frac{K}{2}(\ln(J))^2. \quad (1)$$

Here, $\tilde{I}_1$ is the first deviatoric invariant, $\tilde{\lambda}$ is the deviatoric part of the stretch ratio along the local fiber direction, and J is the determinant of the deformation gradient, F. The matrix strain energy $F_1(\tilde{I}_1)$ was chosen so that $\partial F_1/\partial \tilde{I}_1 = C_1$, yielding the neo-Hookean constitutive model. The derivatives of the fiber strain energy function $F_2(\tilde{\lambda})$ were defined as a function of the fiber stretch:

$$\begin{aligned} \tilde{\lambda}\frac{\partial F_2}{\partial \tilde{\lambda}} &= 0, && \tilde{\lambda} \le 1; \\ \tilde{\lambda}\frac{\partial F_2}{\partial \tilde{\lambda}} &= C_3[\exp(C_4(\tilde{\lambda}-1))-1], && 1 < \tilde{\lambda} < \lambda^*; \\ \tilde{\lambda}\frac{\partial F_2}{\partial \tilde{\lambda}} &= C_5\tilde{\lambda} + C_6, && \tilde{\lambda} \ge \lambda^*. \end{aligned} \quad (2)$$

C_3 scales the exponential stress, C_4 specifies the rate of collagen uncrimping, C_5 is the modulus of straightened collagen fibers, and λ^* is the stretch at which the collagen is straightened. The third term in Equation (1) represents the bulk (volumetric) response, with the bulk modulus K controlling the entire volumetric response of the material. The population-average material coefficients from Gardiner and colleagues were used[22]: $C_1 = 1.44$ MPa, $\lambda^* = 1.062$ (no units), $C_3 = 0.57$ MPa, $C_4 = 48.0$ (no units), and $C_5 = 467.1$ MPa. Population average material coefficients were used because using average coefficients versus subject specific coefficients yielded no significant difference in the accuracy of FE strain predictions.[31] Due to a lack of experimental data describing ligament bulk behavior, the bulk modulus was specified to be two orders of magnitude greater than C_1, yielding nearly incompressible material behavior.[22]

Boundary Conditions

The experimentally measured kinematic dataset was used to prescribe the motion of the tibia relative to the femur in the FE analyses.[22] The coordinates of the kinematic blocks in both the CT and kinematic datasets allowed for correlation of the two datasets. The entire FE model was transformed so that the global coordinate system was aligned with the coordinate system of the femur kinematic block. Motion of the tibia was described using incremental translations and rotations referenced to the femur kinematic block.[30,32] The MCL mesh was attached to the bones by defining node sets, based on the area within the copper wires, at the proximal and distal ends of the MCL as the same rigid material as the femur and tibia, respectively. Contact was enforced using the penalty method.

Finite Element Analysis

The implicitly integrated FE code NIKE3D was used for all analyses.[32] An automatic time stepping strategy was employed, with iterations based on a quasi-Newton method. Each analysis was performed in three parts. In the first part, the knee was moved from the position in which it was placed at the time of the CT scan to the initial testing position (either 0° or 30° of flexion). During the second part, the experimentally measured in situ strains for a given flexion angle and injury state were applied to the MCL. During the third part the experimental kinematic motion was applied (either anterior translation or valgus rotation). FE results were analyzed with GRIZ.[33]

Regional Strains, Insertion Site, and Contract Forces

FE predicted fiber stretches for nodes within each measurement region were averaged and compared to the experimentally measured values. The magnitude of ligament forces at the insertion sites and the magnitude of the resultant forces due to MCL–bone contact were obtained from the NIKE3D output.

Statistical Analysis

Regression analyses were used to evaluate the ability of the FE models to predict experimentally measured values of MCL fiber stretch. FE predictions of regional fiber stretch were determined as a function of location along the length of the MCL. The predicted stretches were calculated and tabulated for all six knees according to test case and compared to experimental results. Coefficients of determination (R^2), regression lines, and p values were determined.

The effect of tibial axial rotation constraint on insertion site and contact forces was assessed with a paired t-test using all the force data (insertion site and contact forces for both test cases at both angles and both loading conditions). The effects of within-subject treatment (test case and flexion angle) in response to anterior and valgus loading on insertion site and contact forces were assessed using two-way repeated measures ANOVAs. The paired t-tests showed no significant effect of tibial constraint on insertion site and contact forces (see Results section), so only the force data for the tests with constrained tibial axial rotation were used in the two-way ANOVAs. In cases when significances were found ($p < 0.05$), multiple comparisons were performed using the Tukey procedure.

RESULTS

Experimental Kinematics

Before ACL resection, the average anterior displacements at 0° and 30° knee flexion in response to a 100 N anterior tibial load were 6.8 ± 2.6 mm and 6.7 ± 2.2 mm, respectively. ACL transection significantly increased anterior displacement in response to a 100 N anterior tibial load (16.5 ± 6.1 mm and 20.8 ± 4.4 mm at 0° and 30°, respectively; $p < 0.001$ for both flexion angles). Before ACL transection, the average valgus rotation at 0° and 30° knee flexion in response to a 10 N-m valgus torque were $3.6° \pm 1.8°$ and $5.1° \pm 2.0°$, respectively. ACL transection did not significantly change valgus rotation in response to a 10 N-m valgus torque ($4.3° \pm 1.9°$ and $5.3° \pm 1.7°$ at 0° and 30°, respectively). Subsequent separation of the medial meniscus attachment had no significant effect on knee joint kinematics for both A-P and V-V loading (data not shown). Because no change in joint kinematics occurred following separation of the medial meniscus from the MCL in the ACL-deficient knee, these data were not subsequently analyzed via FE analysis.

FE Predictions of Regional Fiber Stretch

The FE values for fiber stretch were excellent predictors of experimental fiber stretch with a coefficient of determination of $R^2 = 0.953$ ($p = 0.001$) for all regions, knees, and test cases (Fig. 3). Fringe plots of the FE fiber strain illustrated strain patterns and increases in strain caused by ACL deficiency in response to anterior and valgus loading (Fig. 4). For both types of load

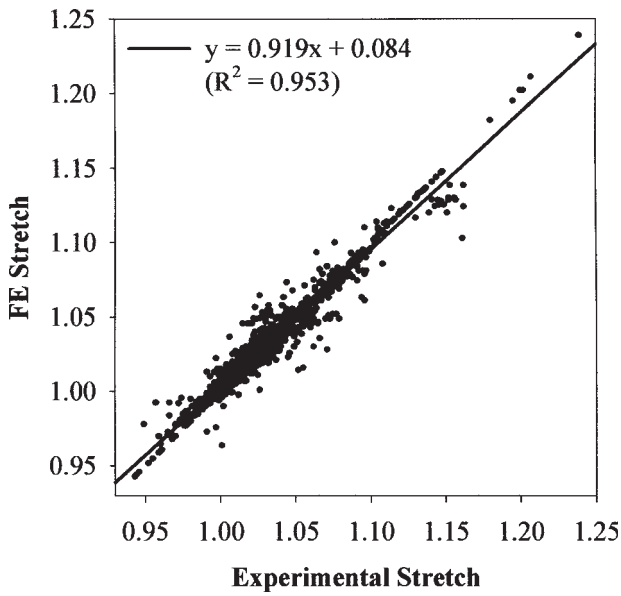

Figure 3. FE predicted versus experimental fiber stretch for all knees, test conditions, and measurement regions ($N = 1632$).

 DOI 10.1002/jor

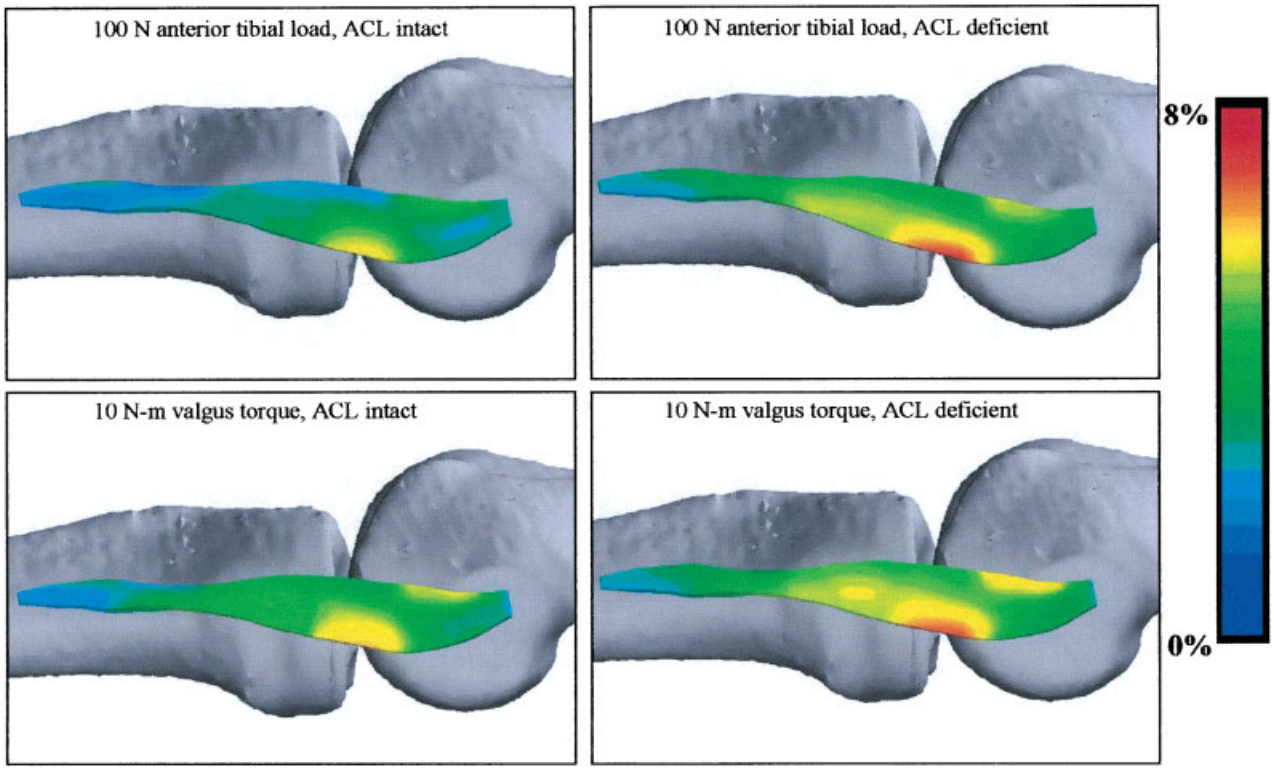

Figure 4. Representative fringe plots of FE predicted fiber strain for a 100 N anterior load (top row) and a 10 N-m valgus load (bottom row) for the uninjured knee and the ACL-deficient knee. MCL strains increased in response to anterior tibial loading when the ACL was injured. MCL strains also increased locally in the ACL-deficient knee in response to a valgus torque, but these local increases did not result in significant changes in insertion site or contact forces.

and regardless of test case, the highest strains were found in the posteriorproximal region.[34] MCL strain increased significantly in response to anterior loading when the ACL was transected, but not in response to a valgus load. Higher MCL strains were more distributed in response to valgus loading than anterior loading regardless of test case. A comprehensive set of MCL strain and kinematics data can be found in Lujan and colleagues.[34]

Tibial Axial Rotation Constraint

A paired *t*-test using all insertion site and contact forces for both flexion angles and loading conditions showed no effect of tibial axial rotation constraint on the predicted forces ($p = 0.154$).

Insertion Site Force

ACL deficiency caused significant increases in both femoral and tibial MCL insertion site forces during anterior tibial translation. The forces were significantly higher at 0° than at 30° in ACL-deficient knees with the 100 N anterior tibial load. The femoral insertion site forces corresponding to the in situ strains in the intact knee (before application of the experimental kinematics) were 39.7 ± 38.1 N and 6.0 ± 5.4 N at 0° and 30°, respectively; the tibial insertion site forces were 42.9 ± 43.1 N and 6.0 ± 5.5 N at 0° and 30°, respectively. Before ACL transection, the femoral insertion site forces during anterior translation were 55.9 ± 38.2 N and 8.3 ± 5.4 N at 0° and 30°, respectively; the tibial insertion site forces were 58.7 ± 42.0 N and 8.3 ± 5.5 N, respectively (Fig. 5, left panel). ACL-deficiency significantly increased femoral (126.6 ± 84.8 N and 74.1 ± 57.8 N at 0° and 30°, respectively) and tibial (133.9 ± 88.5 N and 80.9 ± 62.4 N at 0° and 30°, respectively) insertion site forces during anterior tibial translation ($p < 0.05$ for all cases). Insertion site forces were significantly higher at 0° than at 30° during anterior tibial translation ($p = 0.012$ for both insertions).

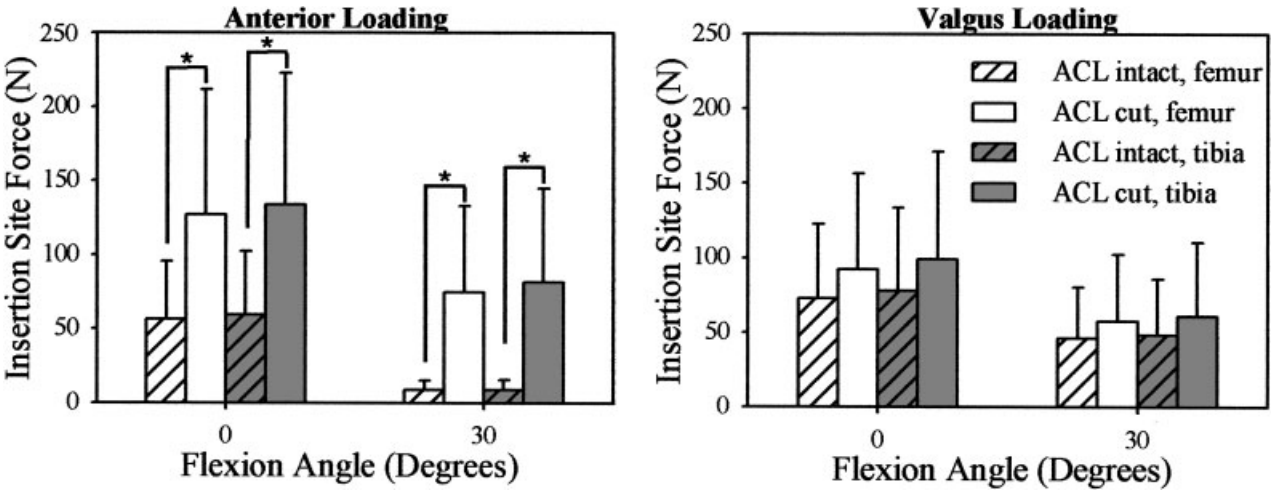

Figure 5. FE predictions of insertion site forces for femoral and tibial insertion sites as a function of flexion angle and ACL state. (Left panel) Anterior tibial translation. (Right panel) Valgus rotation. Asterisks indicate statistically significant comparisons. There was a significant increase in MCL insertion site forces at the femur and tibia during anterior tibial translation after ACL injury at both 0° and 30°. In contrast, there was no significant effect of ACL deficiency on MCL insertion site forces in response to valgus loading. Both tibial and femoral insertion site forces were significantly higher at 0° than at 30° in the ACL-deficient knee during anterior tibial translation (mean ± standard deviation).

In contrast to the anterior loading, ACL deficiency did not significantly affect femoral and tibial insertion site forces during application of valgus torque (Fig. 5, right panel) at either flexion angle. Although the increases were not significant, they followed the same trend as with anterior loading, with higher forces and increases in forces at the tibial insertion and at 0° flexion. Before ACL transection, the femoral insertion site forces during valgus rotation were 72.8 ± 49.9 N and 46.0 ± 34.4 N at 0° and 30°, respectively. Before ACL transection, the tibial insertion site forces during valgus rotation were 77.8 ± 55.6 N and 47.9 ± 37.9 N at 0° and 30°, respectively. After ACL transection, the femoral insertion site forces during valgus rotation were 92.0 ± 64.0 N and 57.5 ± 45.0 N at 0° and 30°, respectively, and the tibial insertion site forces were 99.0 ± 72.2 N and 60.7 ± 49.3 N, respectively.

Contact Forces

ACL deficiency resulted in significantly increased MCL contact forces on the tibia during anterior tibial translation at both flexion angles, and MCL contact forces on the tibia were significantly higher at 0° than at 30° in the ACL-deficient knee. Before ACL transection, the contact forces on the tibia during anterior translation were 11.6 ± 11.9 N and 0.7 ± 0.9 N at 0° and 30°, respectively (Fig. 6, left panel). ACL deficiency significantly increased contact forces (28.4 ± 18.9 N and 21.1 ± 15.8 N at 0° and 30°, respectively) during anterior translation ($p = 0.001$ at both angles). MCL contact forces on the tibia in the ACL-deficient knee were significantly higher at 0° than at 30° in response to anterior tibial loading ($p = 0.044$). ACL deficiency did not significantly affect contact forces during application of valgus torque (Fig. 6, right panel).

DISCUSSION

Our hypothesis was that ACL deficiency would increase MCL insertion site forces at the femur and tibia and increase contact forces between the MCL and the bones in response to both anterior and valgus loading. This hypothesis was partially disproved. In the ACL-deficient knee, the MCL is indeed subjected to higher insertion site and contact forces in response to an anterior load. However, MCL forces due to a valgus torque are not significantly increased in the ACL-deficient knee. It follows that the MCL resists anterior

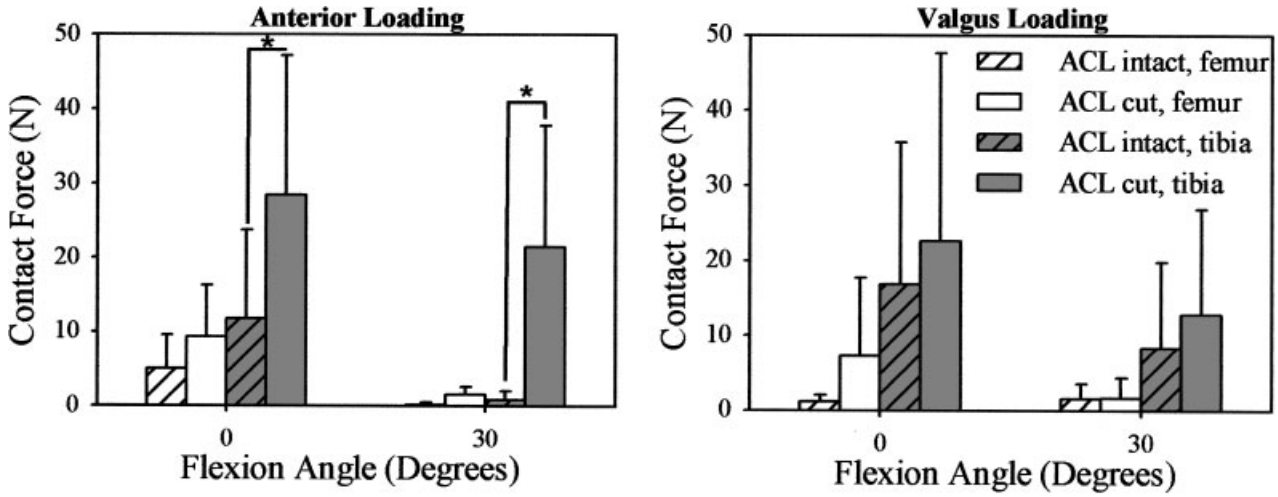

Figure 6. FE predictions of contact forces between the MCL and femur and between the MCL and tibia as a function of flexion angle and ACL injury state. (Left) Anterior tibial translation. (Right) Valgus rotation. Asterisks indicate statistically significant comparisons. ACL deficiency significantly increased tibial contact forces at both flexion angles during anterior tibial translation. Further, tibial contact forces in the ACL-deficient knee at 0° were significantly higher than at 30° during anterior loading. In contrast, there was no significant effect of ACL deficiency on MCL contact forces during valgus loading (mean ± standard deviation).

tibial translation in knees with intact ACLs, but the ACL is not a restraint to valgus rotation when a healthy MCL is present.

ACL deficiency caused a significant increase in MCL insertion site and contact forces in response to anterior tibial loading. This result is supported by an FE study[35] and by cadaver studies that utilized a robotic/universal force-moment sensor system to calculate MCL insertion site forces in the ACL-deficient knee.[16,17] Moglo and colleagues created an FE model including the MCL, ACL, posterior cruciate ligament (PCL), lateral collateral ligament (LCL), menisci, and cartilage.[35] A 100 N posterior load was applied to the femur at flexion angles from 0° to 90°. At full extension, forces in collateral ligaments increased in the ACL-deficient knee. Better support for our findings can be found in the cadaver studies.[16,17] In both studies, anterior loads were applied to intact and ACL-deficient cadaver knees and the resulting MCL insertion site forces were measured. A significant increase in MCL insertion site forces occurred during anterior tibial loading in the ACL-deficient knee.

In vivo studies have demonstrated that MCL healing is inferior when injured in conjunction with the ACL.[2–4,12] Knee laxity increased and MCL material properties decreased when the MCL was injured in conjunction with the ACL as compared to MCL injury with intact ACL, but only one study measured MCL forces. Using a goat model, the insertion site forces in healing MCLs in response to an anterior tibial load in knees with reconstructed ACLs were measured by Abramowitch and colleagues using a robotic/universal force-moment sensor system.[2] They concluded that "the healing MCL may have been required to take on excessive loads and was unable to heal sufficiently as compared to an isolated MCL injury" (p. 1124). Although these conclusions were based on animal data, our results suggest that differences in healing could be due to either anterior or valgus loading. The insertion site forces with a valgus torque were generally of the same magnitude for a given flexion angle as the insertion site forces in response to an anterior load, though they did not significantly increase with ACL deficiency, and the types and magnitudes of loads that hinder MCL healing are unknown.

The ACL is not a restraint to valgus rotation if the MCL is intact (Figs. 4 and 5, right panels). At first this may seem contradictory to the widely held notion that the ACL is a secondary restraint to valgus rotation.[2–4,7,8,10,11] However, this conclusion is based on results with MCL transection. Specifically, when the MCL was injured or transected, the ACL experienced increased loading during application of a valgus torque. Although

our conclusion has not been reported previously, results from other studies support the conclusions indirectly. Engle and colleagues examined the effect of ACL repair and graft restructuring on MCL healing after an O'Donoghue triad injury.[4] Between 0 and 12 weeks postoperatively, anterior laxity increased significantly, but valgus laxity did not. Markolf and coworkers found that valgus knee laxity was unaffected by sectioning the cruciate ligaments.[14] This idea is further supported by Grood and colleagues,[13] who found that the ACL and PCL combined accounted for only 14.8% of the medial restraining moment at 5° knee flexion and only 13.4% of the restraining moment at 25° knee flexion. Thus, when evaluating valgus laxity in the ACL-injured knee, any increase in valgus laxity indicates a compromised MCL.

Applying in situ strain to the MCL during the second part of the FE analysis creates insertion site forces. These forces represent the MCL contribution to knee stability when little or no muscle activation or external loading exists. The forces caused by the in situ strain were smaller than the forces after anterior or valgus loading in the intact knee, although not always significantly, reflecting the relatively low load limits. In the ACL-deficient knee, insertion site forces increased significantly in response to an anterior tibial load, but not a valgus load, from the insertion site forces caused by the in situ strain, following the trend when comparing insertion site forces in the ACL-deficient knee to the intact knee.

Changes in MCL contact forces followed the trend of MCL insertion site forces with a significant increase in contact forces between the MCL and tibia following ACL transection in response to an anterior tibial load, but not a valgus torque. Contact forces were generated between the MCL and tibia during anterior tibial translation as the MCL slid over the convex surface of the tibia. These forces were relatively small in knees with intact ACL, but increased when the ACL was transected, and on average anterior tibial translation was more than doubled, forcing the MCL to slide over parts of the bone that have increased curvature. This is the first study to examine ligament contact forces using subject-specific FE modeling.

The attachment of the medial meniscus to the MCL was not modeled, an approach justified by the results of our previous study, which demonstrated that transection of the attachment had no effect on knee kinematics under valgus loading in the intact knee.[22] In the present study, it was confirmed that loss of attachment of the meniscus had no significant effect on joint kinematics for both A-P and V-V loading in the ACL-deficient knee. Of course, other soft tissue structures that were dissected away may have contributed to knee stability under A-P and V-V loading, and thus as with any cadaveric study, caution should be taken when extrapolating results to other situations.

Improvements in the experimental methods resulted in substantially better agreement between FE predictions and experimental measurements of fiber stretch than was obtained in our previous study.[22] Improvements included use of a more accurate motion analysis system, placement of wires around the insertion sites to identify their locations in CT images, and placement of additional strain markers along and across the MCL.[23] The excellent correlation between experimental and FE predicted fiber strains ($R^2 = 0.953$) provides confidence in the fidelity of the subject-specific FE model predictions. Data such as insertion site forces and contact forces, which elucidate other injury mechanisms and risks, can be evaluated using subject-specific FE methods. Further, the combination of experimental and computational results can be used to determine likely locations of injury and to what extent they may occur.

Assumptions were made in the constitutive model used for the MCL to decrease both the experimental and computational times. Average material coefficients were used, because in a previous study, results using subject-specific material properties were not significantly different from those using average properties.[22] The MCL was also assumed to have homogenous material properties, yielding good correlations between experimental and FE strains.

The A-P and V-V mechanical testing simulated an ideal clinical exam for knee laxity; no attempt was made to simulate weight bearing or muscle forces. The anterior load and valgus torque limits were specifically chosen to allow multiple tests on a single knee. Future research examining other loading conditions including muscle and body weight forces during regular daily activities is still needed.

ACKNOWLEDGMENTS

Financial support from NIH Grant no. AR47369 and from the Campbell Fellowship, through the College of

Engineering at the University of Utah (MSD), is gratefully acknowledged.

REFERENCES

1. Robins AJ, Newman AP, Burks RT. 1993. Postoperative return of motion in anterior cruciate ligament and medial collateral ligament injuries. The effect of medial collateral ligament rupture location. Am J Sports Med 21:20–25.
2. Abramowitch SD, Yagi M, Tsuda E, et al. 2003. The healing medial collateral ligament following a combined anterior cruciate and medial collateral ligament injury—a biomechanical study in a goat model. J Orthop Res 21:1124–1130.
3. Anderson DR, Weiss JA, Takai S, et al. 1992. Healing of the medial collateral ligament following a triad injury: a biomechanical and histological study of the knee in rabbits. J Orthop Res 10:485–495.
4. Engle CP, Noguchi M, Ohland KJ, et al. 1994. Healing of the rabbit medial collateral ligament following an O'Donoghue triad injury: effects of anterior cruciate ligament reconstruction. J Orthop Res 12:357–364.
5. Ichiba A, Nakajima M, Fujita A, et al. 2003. The effect of medial collateral ligament insufficiency on the reconstructed anterior cruciate ligament: a study in the rabbit. Acta Orthop Scand 74:196–200..6.
   Inoue M, McGurk-Burleson E, Hollis JM, et al. 1987. Treatment of the medial collateral ligament injury. I: The importance of anterior cruciate ligament on the varus-valgus knee laxity. Am J Sports Med 15:15–21.
7. Loitz-Ramage BJ, Frank CB, Shrive NG. 1997. Injury size affects long-term strength of the rabbit medial collateral ligament. Clin Orthop 337:272–280.
8. Ma CB, Papageogiou CD, Debski RE, et al. 2000. Interaction between the ACL graft and MCL in a combined ACL + MCL knee injury using a goat model. Acta Orthop Scand 71:387–393.
9. Mazzocca AD, Nissen CW, Geary M, et al. 2003. Valgus medial collateral ligament rupture causes concomitant loading and damage of the anterior cruciate ligament. J Knee Surg 16:148–151.
10. Norwood LA, Cross MJ. 1979. Anterior cruciate ligament: functional anatomy of its bundles in rotatory instabilities. Am J Sports Med 7:23–26.
11. Woo SL, Jia F, Zou L, et al. 2004. Functional tissue engineering for ligament healing: potential of antisense gene therapy. Ann Biomed Eng 32:342–351.
12. Woo SL, Young EP, Ohland KJ, et al. 1990. The effects of transaction of the anterior cruciate ligament on healing of the medial collateral ligament. A biomechanical study of the knee in dogs. J Bone Joint Surg Am 72:382–392.
13. Grood ES, Noyes FR, Butler DL, et al. 1981, Ligamentous and capsular restraints preventing straight medial and lateral laxity in intact human cadaver knees. J Bone Joint Surg Am 63:1257–1269.
14. Markolf KL, Mensch JS, Amstutz HC. 1976. Stiffness and laxity of the knee—the contributions of the supporting structures. A quantitative in vitro study. J Bone Joint Surg Am 58:583–594.
15. Butler DL, Noyes FR, Grood ES. 1980. Ligamentous restraints to anterior-posterior drawer in the human knee. A biomechanical study. J Bone Joint Surg Am 62:259–270.
16. Kanamori A, Sakane M, Zeminski J, et al. 2000. In-situ force in the medial and lateral structures of intact and ACL-deficient knees. J Orthop Sci 5: 567–571.
17. Sakane M, Livesay GA, Fox RJ, et al. 1999. Relative contribution of the ACL, MCL, and bony contact to the anterior stability of the knee. Knee Surg Sports Traumatol Arthrosc 7:93–97.
18. Seering WP, Piziali RL, Nagel DA, et al. 1980. The function of the primary ligaments of the knee in varus-valgus and axial rotation. J Biomech 13: 785–794.
19. Miyasaka KC, Daniel DM, Stone ML, et al. 1991. The incidence of knee ligament injuries in the general population. Am J Knee Surg 4:3–8.
20. Fetto JF, Marshall JL. 1978. Medial collateral ligament injuries of the knee: a rationale for treatment. Clin Orthop 132:206–218.
21. Hull ML. 1997. Analysis of skiing accidents involving combined injuries to the medial collateral and anterior cruciate ligaments. Am J Sports Med 25: 35–40.
22. Gardiner JC, Weiss JA. 2003. Subject-specific finite element analysis of the human medial collateral ligament during valgus knee loading. J Orthop Res 21:1098–1106.
23. Lujan TJ, Lake SP, Plaizier TA, et al. 2005. Simultaneous measurement of three-dimensional joint kinematics and ligament strains with optical methods. ASME J Biomech Eng 127:193–197.
24. Gardiner JC. 2002. Computational modeling of ligament mechanics (Ph.D. dissertation). Salt Lake City, UT: Department of Bioengineering, University of Utah.
25. Grood ES, Suntay WJ. 1983. A joint coordinate system for the clinical description of the three-dimensional motions: application to the knee. J Biomech Eng 105:136–144.
26. Gardiner JC, Weiss JA. 2001. Simple shear testing of parallel-fibered planar soft tissues. J Biomech Eng 123:170–175.

27. Weiss JA, Gardiner JC, Ellis BJ, et al. Three-dimensional finite element modeling of ligaments: technical aspects. Med Eng Phys (in press).
28. Boissonnat JD. 1998. Shape reconstruction from planar cross-sections. Comput Vis Graphics Image Process 44:1–29.
29. Schroeder WJ, Zarge J, Lorensen WE. 1992. Decimation of triangle meshes. Comp Graph (Proc SIGGRAPH) 25.
30. Maker BN. 1995. Rigid bodies for metal forming analysis with NIKE3D. Lawrence Livermore Lab Rept UCRL-JC-119862:1–8.
31. Weiss JA, Maker BN. 1996. Finite element implementation of incompressible, transversely isotropic hyperelasticity. Comput Methods Appl Mech Eng 135:107–128.
32. Maker BN. 1995. NIKE3D: a nonlinear, implicit, three-dimensional finite element code for solid and structural mechanics. Lawrence Livermore Lab Tech Rept UCRL-MA-105268.
33. Speck D. 2001. GRIZ - Finite element analysis results visualization for unstructured grids–user manual. Lawrence Livermore National Laboratory UCRL-MA-115696 Rev.2.
34. Lujan TJ, Dalton MS, Thompson BM, et al. 2005. MCL strains and joint kinematics in the ACL-deficient and posteromedial meniscus injured knee. Am J Sports Med (in press).
35. Moglo KE, Shirazi-Adl A. 2003. Biomechanics of passive knee joint in drawer: load transmission in intact and ACL-deficient joints. Knee 10:265–276.